Revised Version

DESY-08-057
OUTP-08-13-P

Angular correlations in multi-jet final states from $k_\perp$-dependent parton showers

F. Hautmann[1] and H. Jung[2]
[1] *Theoretical Physics Department, University of Oxford, Oxford OX1 3NP*
[2] *Deutsches Elektronen Synchrotron, D-22603 Hamburg*

Abstract

We investigate parton-branching methods based on transverse-momentum dependent (TMD) parton distributions and matrix elements for the Monte Carlo simulation of multi-particle final states at high-energy colliders. We observe that recently measured angular correlations in ep final states with multiple hadronic jets probe QCD coherence effects in the space-like branching, associated with finite-angle gluon radiation from partons carrying small longitudinal momenta, and not included in standard shower generators. We present Monte Carlo calculations for azimuthal two-jet and three-jet distributions, for jet multiplicities and for correlations in the transverse-momentum imbalance between the leading jets. We discuss comparisons with current experimental multi-jet data, and implications of corrections to collinear-ordered showers for LHC final states.

arXiv:0805.1049v3 [hep-ph] 24 Sep 2008

I. INTRODUCTION

Hadronic final states containing multiple jets have been investigated at the Tevatron and HERA colliders, and will play a central role in the Large Hadron Collider (LHC) physics program. The interpretation of experimental data for such final states relies both on perturbative multi-jet calculations (see [1] for a recent overview) and on realistic event simulation by parton-shower Monte Carlo generators (see e.g. [2–4]).

Owing to the complex kinematics involving multiple hard scales and the large phase space opening up at very high energies, multi-jet events are potentially sensitive to effects of QCD initial-state radiation that depend on the finite transverse-momentum tail of partonic matrix elements and distributions. For an overview see [5]. In perturbative multi-jet calculations truncated to fixed order in α_s [1], finite-$k_\perp$ contributions are taken into account partially, order-by-order, through higher-loop corrections. This is generally sufficient for inclusive jet cross sections, but likely not for more exclusive final-state observables.

On the other hand, standard shower Monte Carlos reconstructing exclusive events, such as HERWIG [6] and PYTHIA [7], are based on collinear evolution of the initial-state jet. Finite-$k_\perp$ contributions are not included, but rather correspond to corrections [8–10] to the angular or transverse-momentum ordering implemented in the parton-branching algorithms. The theoretical framework to take these corrections into account is based on using initial-state distributions (pdfs) unintegrated in both longitudinal and transverse momenta [10], coupled to hard matrix elements (ME) suitably defined off mass shell. See e.g. [11] for discussion of the Monte Carlo shower implementation of the method. Event generators based on $k_\perp$-dependent showers of this kind include [12–15]. These generators are not as developed as standard Monte Carlos like HERWIG and PYTHIA. However, they have the potential advantage of a more accurate treatment of the space-like parton shower at high energy.

Collinear-based shower generators like HERWIG and the new PYTHIA contain the effects of color coherence for soft gluon emission from partons carrying longitudinal momentum fraction $x \sim \mathcal{O}(1)$. However as the energy increases and emissions that are not collinearly ordered become more important, coherence effects from space-like partons carrying momentum fractions $x \ll 1$ set in. These small-x coherence effects are not included in HERWIG or PYTHIA but are included in $k_\perp$-dependent parton showers, and characterize the structure of the initial-state branching at very high energies.

This paper examines how corrections to space-like parton showers affect properties of final state jet correlations and associated distributions. We study azimuthal correlations and transverse-momentum correlations for multi-jet processes. We obtain numerical Monte Carlo results for collinear and $k_\perp$-dependent parton showers, and use the precise experimental data on tri-jets in ep collisions that have recently become available [16]. We observe significant corrections arising from regions [5] with three well-separated hard jets in which the partonic lines along the decay chain in the initial state are not ordered in transverse momentum. These give rise to quite distinctive features in the jet angular correlations.

Besides jet final states, the coherence effects from highly off-shell processes discussed in this paper affect a variety of different final states at high energy. A significant example concerns the associated production of heavy flavors and heavy bosons at the LHC with two high-p_t jets. We come back to this at the end of the paper in Sec. V.

The paper is structured as follows. We begin in Sec. II by describing experimental results on multi-jet correlations. In Sec. III we recall basic aspects on the implementation

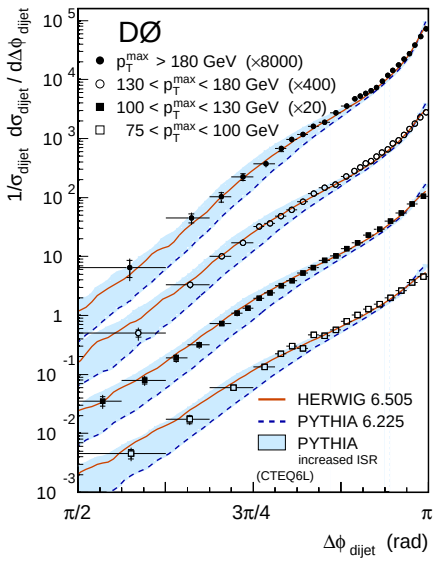

FIG. 1: Dijet azimuthal correlations measured by D0 along with the HERWIG and PYTHIA results [17].

of transverse-momentum dependent pdfs and MEs in parton-branching algorithms. We then compute angular correlations in three-jet final states by $k_\perp$-dependent Monte Carlo showering. We compare the results with HERWIG and with experimental data. We consider correlations in the azimuthal angle between the two hardest jets, and further analyze the distribution of the third jet. We investigate in particular the quantitative effect of the finite high-$k_\perp$ tail in the hard ME. In Sec. IV we present results for jet multiplicity distributions and for momentum correlations. In Sec. V we discuss prospects for LHC final states and give conclusions. Some details on u-pdf fits and on time-like showering effects are left to Appendix A and Appendix B.

II. MEASUREMENTS OF FINAL-STATE JET CORRELATIONS

In this section we recall experimental results from Tevatron and HERA on angular correlations in multi-jet production.

In a multi-jet event the correlation in the azimuthal angle $\Delta\phi$ between the two hardest jets provides a useful measurement, sensitive to how well QCD multiple-radiation effects are described. In leading order one expects two back-to-back jets; higher-order radiative contributions cause the $\Delta\phi$ distribution to spread out. At the LHC, measurements of $\Delta\phi$ distributions in multi-jet events may become accessible relatively early, and be used to test the Monte Carlo description of the events.

Fig. 1 [17] shows the Tevatron $\Delta\phi$ measurements. The data are compared with HERWIG and PYTHIA results. The data are found [17, 18] to have little sensitivity to final-state showering parameters and to be in contrast very sensitive to initial-state showering parameters. In particular, they have been used for re-tuning of these parameters in PYTHIA [18]. A reasonably good description of the measurements by Monte Carlo is obtained.

On the other hand, the HERA $\Delta\phi$ measurements [16, 19, 20] are not so well described by the standard HERWIG and PYTHIA Monte Carlo showers in most of the data kinematic

range. We will discuss more on this below. These measurements are characterized by the large phase space available for jet production and relatively small values of the ratio between the jet transverse momenta and center-of-mass energy. For these reasons, despite the much lower energy at HERA, they may be just as relevant as the Tevatron data for extrapolation of initial-state showering effects to the LHC.

In the rest of this section we focus on the recent, precise ep measurements [16] of jet correlations, and discuss potential sources of large QCD corrections.

In Ref. [16] the ZEUS collaboration have presented data for two-jet and three-jet production associated with

$$Q^2 > 10 \text{ GeV}^2 \quad , \qquad 10^{-4} < x < 10^{-2} \quad , \tag{1}$$

and performed a comparison with next-to-leading-order calculations [21]. ZEUS measured differential distributions as functions of jet transverse energy and pseudorapidity as well as correlations in azimuthal angles and transverse momenta. The selection cuts on the jet phase space are given by

$$E_{T,HCM}^{\text{jet}-1} > 7 \text{ GeV} \quad , \qquad E_{T,HCM}^{\text{jet}-2,3} > 5 \text{ GeV} \quad , \qquad -1 < \eta_{lab} < 2.5 \quad , \tag{2}$$

where $E_{T,HCM}$ are the jet transverse energies in the hadronic center-of-mass frame, and η_{lab} are the jet pseudorapidities in the laboratory frame. The overall agreement of data with NLO results is within errors [16]. However, while inclusive jet rates are reliably predicted by NLO perturbation theory, jet correlations turn out to be affected by large theoretical uncertainties at NLO. Results from [16] for di-jet distributions are reproduced in Fig. 2 for easier reference.

The plot at the top in Fig. 2 shows the x-dependence of the di-jet distribution integrated over $\Delta\phi < 2\pi/3$, where $\Delta\phi$ is the azimuthal separation between the two high-E_T jets. The plot at the bottom shows the di-jet distribution in $\Delta\phi$ for different bins of x. We see that the variation of the predictions from order-α_s^2 to order-α_s^3 is significant. In the azimuthal correlation for a given x bin, the variation increases with decreasing $\Delta\phi$. In the distribution integrated over $\Delta\phi$, the variation increases with decreasing x. The lowest order, where the differential cross section $d\sigma/d\Delta\phi$ is non-trivial, is $\mathcal{O}(\alpha_s^2)$ and the NLO calculation is labeled with $\mathcal{O}(\alpha_s^3)$.

Given the large difference between order-α_s^2 and order-α_s^3 results, it seems to be questionable to estimate the theoretical uncertainty at NLO from the conventional method of varying the renormalization/factorization scale.

Besides angular distributions, a behavior similar to that described above is also found in [16] for other associated distributions such as momentum correlations.[1] We will come back to this in Sec. IV.

Note that the Tevatron $\Delta\phi$ distribution in Fig. 1 drops by two orders of magnitude over a fairly narrow range, essentially still close to the two-jet region. The measurement is dominated essentially by leading-order processes. Not surprisingly the Monte Carlos provide a good description of the data. In Fig. 2 a comparable two order of magnitude drop occurs over the whole $\Delta\phi$ range. Much more QCD dynamics than leading order is probed.

The stability of predictions for the jet observables under consideration in Fig. 2 depends on a number of physical effects. Part of these concern the jet reconstruction and hadronization. The ZEUS [16] and H1 [19, 20] jet algorithm has moderate hadronization corrections [22]

[1] On the other hand, NLO results are much more stable in the case of inclusive jet cross sections [16].

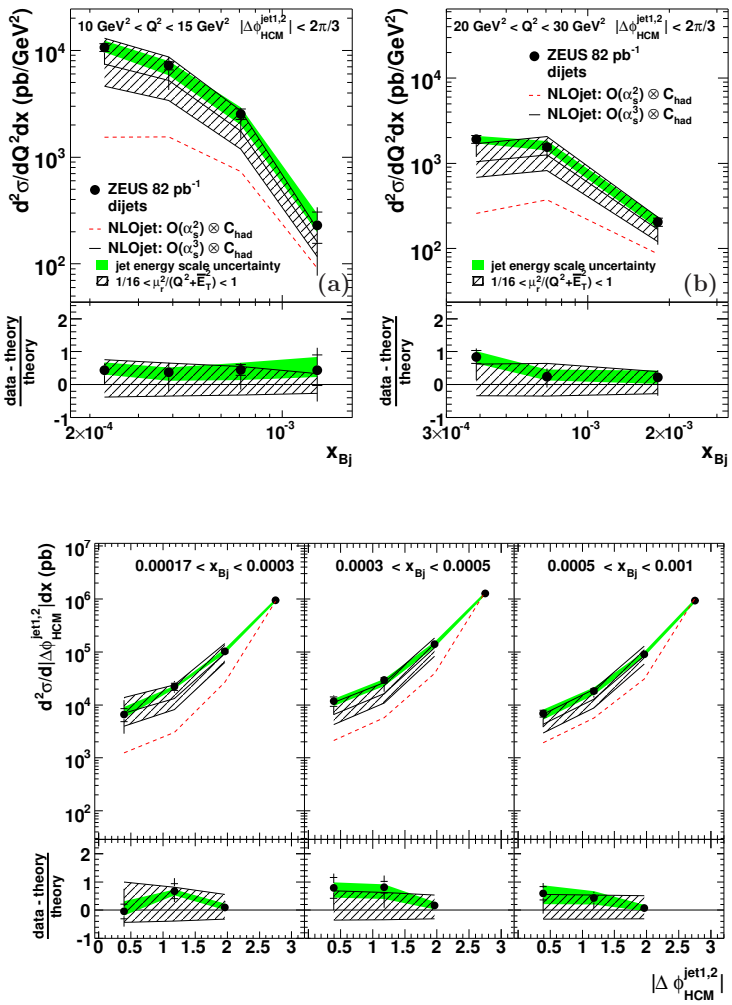

FIG. 2: (top) Bjorken-x dependence and (bottom) azimuth dependence of di-jet distributions at HERA as measured by ZEUS [16].

and is free of nonglobal single-logarithmic components [23]. The kinematic cuts [16] on the hardest jet transverse momenta are set to be asymmetric, so as to avoid double-logarithmic contributions in the minimum p_T [24]. Note that $Q^2 > 10$ GeV^2 (Eq. (1)), and nonperturbative corrections affecting the jet distributions at the level of inverse powers of Q are expected to be moderate.

Further effects concern radiative corrections at higher order. Fixed-order calculations beyond NLO are not within present reach for multi-jet processes in ep and pp collisions. Resummed calculations of higher-order logarithmic contributions from multiple infrared emissions are performed with next-to-leading accuracy in [25]. These contributions are enhanced in the region where the two high-E_T jets are nearly back-to-back. Multiple infrared emissions are also taken into account by parton-branching methods in shower Monte Carlos such as HERWIG [6]. Note however that important corrections in Fig. 2 arise for decreasing $\Delta\phi$, where the two jets are not close to back-to-back and one has effectively three well-separated hard jets [5]. The corrections increase as x decreases. Effects analogous to those in Fig. 2 are seen in the ZEUS results for the three-jet cross section, shown in Fig. 3 [16], particu-

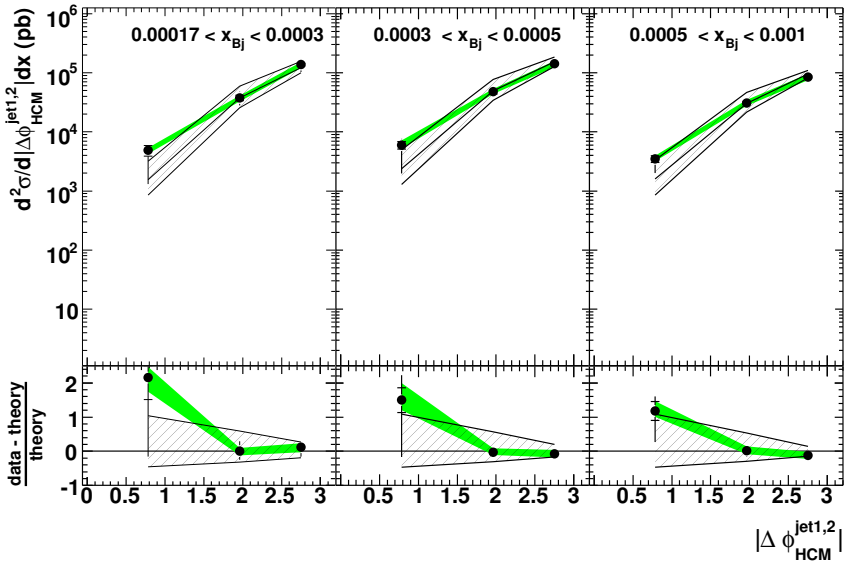

FIG. 3: Three-jet cross section versus azimuthal separation between the two highest-E_T jets as measured by ZEUS [16].

larly for the small-$\Delta\phi$ and small-x bins.[2] In Sec. III we analyze the angular distribution of the third jet, and find significant contributions for small $\Delta\phi$ from regions of the space-like shower where the transverse momenta in the initial-state decay chain are not ordered. These contributions are not fully taken into account either by fixed-order calculations truncated to NLO or by parton showers implementing collinear ordering such as HERWIG and PYTHIA.

In the next section we present the results of computing jets' angular correlations by parton-shower methods that include finite-$k_\perp$ corrections to collinear ordering. We compare these results with the collinear-based shower HERWIG, and with experimental data.

III. ANGULAR CORRELATIONS FROM $K_\perp$ SHOWER MONTE CARLO

Corrections to the collinear ordering in the space-like shower can be incorporated in Monte Carlo event generators by implementing transverse-momentum dependent (TMD) parton distributions (unintegrated pdfs) and matrix elements (ME) through high-energy factorization [10]. This method allows parton distributions at fixed $k_\perp$ to be defined gauge-invariantly for small x. Basic aspects of the parton-shower implementation of the method are discussed in [11]. In this section we start by briefly recalling the basis for the introduction of unintegrated pdfs (u-pdfs) at high energy; we comment on generalizations relevant for low energies and general-purpose tools; then we apply the $k_\perp$-dependent parton branching to the study of angular jet correlations.

[2] The error band for the theory curves in Fig. 3 [16] is obtained by varying the value of the renormalization scale from $(Q^2 + \overline{E}_T^2)$ to $(Q^2 + \overline{E}_T^2)/16$, where $\overline{E}_T$ is the average E_T of the three hardest jets in each event.

A. Unintegrated pdfs

To characterize a transverse-momentum dependent parton distribution gauge-invariantly over the whole phase space is a nontrivial question [26, 27], currently at the center of much activity. See overview in [5]. In the case of small x a well-prescribed, gauge-invariant definition emerges from high-energy factorization [10], and has been used for studies of collider processes both by Monte Carlo (see reviews in [5, 28]) and by semi-analytic resummation approaches (see [29, 30]).

The diagrammatic argument for gauge invariance, given in [10], and developed in [31], is based on relating off-shell matrix elements with physical cross sections at $x \ll 1$, and exploits the dominance of single gluon polarization at high energies.[3] The main reason why a natural definition for TMD pdfs can be constructed in the high-energy limit is that one can relate directly (up to perturbative corrections) the cross section for a *physical* process, say, photoproduction of a heavy-quark pair, to an *unintegrated* gluon distribution, much as, in the conventional parton picture, one does for DIS in terms of ordinary (integrated) parton distributions. On the other hand, the difficulties in defining a TMD distribution over the whole phase space can largely be associated with the fact that it is not obvious how to determine one such relation for general kinematics.

The evolution equations obeyed by TMD distributions defined from the high-energy limit are of the type of energy evolution [32]. Factorization formulas in terms of TMD distributions [10] have corrections that are down by logarithms of energy rather than powers of momentum transfer. On the other hand, it is important to observe that this framework allows one to describe the ultraviolet region of arbitrarily high $\mathrm{k}_\perp$ and in particular re-obtain the structure of QCD logarithmic scaling violations [29–31]. This ultimately justifies the use of this approach for jet physics. In particular it is the basis for using corresponding Monte Carlo implementations [11–15, 33] to treat multi-scale hard processes at the LHC.

From both theoretical and phenomenological viewpoints, it is one of the appealing features of the high-energy framework for TMD distributions that one can relate its results to a well-defined summation of higher-order radiative corrections. By expanding these results to fixed order in α_s, one can match the predictions thus obtained against perturbative calculations. This has been verified for a number of specific processes at next-to-leading order (see for instance [34] for heavy flavor production) and more recently at next-to-next-to-leading order (see for instance [35]). Note that this fact also provides the basis for shower algorithms implementing this framework to be combined with fixed-order NLO calculations by using existing techniques for such matching.

Later in this section we use Monte Carlo implementing the high-energy definition of u-pdfs to analyze jet production. Before doing this, we comment briefly on open issues and generalizations to low energies.

B. Comments on unintegrated pdfs beyond low x

In the general case, factorization formulas in terms of unintegrated parton distributions will have a considerably complex structure [26]. Full results are yet to be established. A

[3] It is emphasized e.g. in [27, 28] that a fully worked out operator argument, on the other hand, is highly desirable but is still missing.

prototypical calculation that illustrates this structure is carried out in [36], which treats, rather than a general scattering observable, a simpler problem, the electromagnetic form factor of a quark. This case is however sufficient to illustrate certain main features, in particular the role of nonperturbative, gauge-invariantly defined factors associated with infrared subgraphs (both collinear and soft), and the role of infrared subtractive techniques that serve to identify these factors. See also [37] for recent analyses along these lines for more general processes involving fully unintegrated pdfs.

One of the questions that a full factorization statement will address is the treatment of soft gluons exchanged between subgraphs in different collinear directions. The underlying dynamics is that of non-abelian Coulomb phase, treated a long time ago in [38] for the fully inclusive Drell-Yan case. But a systematic treatment for more complex observables, including color in both initial and final states, is still missing, as emphasized recently in [39–41] for di-hadron and di-jet hadroproduction near the back-to-back region.[4]

A further question concerns lightcone divergences [26] and the $x \to 1$ endpoint behavior. The singularity structure at $x \to 1$ is different in the TMD case than for ordinary (integrated) distributions, giving divergences even in dimensional regularization with an infrared cut-off [43]. The singularities can be understood in terms of gauge-invariant eikonal-line matrix elements [43], and the TMD behavior can be related to cusp anomalous dimensions [44, 45] and lack of complete KLN cancellations [46]. In general this affects the precise form of factorization and relation with collinear distributions.

Applications of u-pdfs at low energies include semi-inclusive leptoproduction ([47–49], and references therein), spin asymmetries [50], exclusive reactions [51]. In these cases infrared subtractive techniques of the type [36, 52] serve for TMD-factorization calculations [53] and in particular for the proper treatment of overlapping momentum regions.[5] At high-energy colliders, general characterizations of TMD distributions will be relevant for turning present $\mathrm{k}_\perp$-showering generators into general-purpose tools to describe hadronic final states over the whole phase space [5, 60].

In the rest of this section we will consider applications of $\mathrm{k}_\perp$-shower generators to multi-jet final states. The main focus is on regions where jets are far from back-to-back, and the total energy is much larger than the transferred momenta so that the values of x are small. In this regime the ambiguities related to soft Coulomb exchange and to lightcone divergences are not expected to be crucial. We will find that the TMD distributions, as well as the transverse-momentum dependence of short-distance matrix elements, play a very essential role to describe correlations in angle and momentum of the jets.

C. $k_\perp$ shower with u-pdfs

Monte-Carlo event generators based on unintegrated pdfs use factorization at fixed $\mathrm{k}_\perp$ [10] in order to a) generate the hard scattering event, including dependence on the initial trans-

[4] Note that interestingly in [42], which has a different point of view than TMD, Coulomb/radiative mixing terms are found to be responsible for the breaking of angular ordering in the initial-state cascade and the appearance of superleading logarithms in di-jet cross sections with a gap in rapidity.

[5] Subtraction techniques related to those of [36, 52] are developed in [54] for soft-collinear effective theory, and studied in [55] and [56] in relation with standard perturbative methods. See also SCET applications to shower algorithms [57], TMD pdfs [58] and jet event shapes [59] for use of these techniques.

verse momentum, and b) couple this to the evolution of the initial state to simulate the parton cascade. Implementations of this kind include [8, 12–15]. The hard scattering event is generated by $k_\perp$-dependent matrix elements (ME) computed from perturbation theory. Different generators differ by the detailed model for initial state. For the calculations that follow we use the Monte Carlo implementation CASCADE [12].

The hard ME in the Monte Carlo are obtained by perturbative calculation [10], while the u-pdfs are determined from fits to experimental data [33]. The parton-branching equation used for the unintegrated gluon distribution $\mathcal{A}$ is schematically of the form [8, 12, 33]

$$\begin{aligned}\mathcal{A}(x,k_\perp,\mu) &= \mathcal{A}_0(x,k_\perp,\mu) + \int \frac{dz}{z} \int \frac{dq^2}{q^2}\ \Theta(\mu - zq) \\ &\times\ \Delta(\mu,zq)\ \mathcal{P}(z,q,k_\perp)\ \mathcal{A}(\frac{x}{z},k_\perp+(1-z)q,q) \quad . \end{aligned} \tag{3}$$

The first term in the right hand side of Eq. (3) is the contribution of the non-resolvable branchings between starting scale Q_0 and evolution scale μ, and is given by

$$\mathcal{A}_0(x,k_\perp,\mu) = \mathcal{A}_0(x,k_\perp,Q_0)\ \Delta(\mu,Q_0) \quad , \tag{4}$$

where Δ is the Sudakov form factor, and the starting distribution $\mathcal{A}_0(x,k_\perp,Q_0)$ at scale Q_0 is determined from data fits. Details on the starting distribution used for the calculations that follow are given in Appendix A.

The integral term in the right hand side of Eq. (3) gives the $k_\perp$-dependent branchings in terms of the Sudakov form factor Δ and unintegrated splitting function $\mathcal{P}$. The explicit

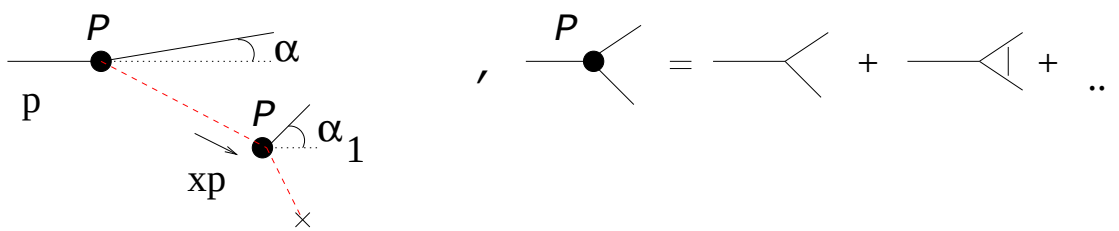

FIG. 4: (left) Coherent radiation in the space-like parton shower for $x \ll 1$; (right) the unintegrated splitting function $\mathcal{P}$, including small-x virtual corrections.

expressions for these factors are specified in [33], and include the effects of coherent gluon radiation not only at large x (as e.g. in HERWIG) but also at small x [9] in the angular region (Fig. 4)

$$\alpha/x > \alpha_1 > \alpha \quad , \tag{5}$$

where the angles α for the partons radiated from the initial-state shower are taken with respect to the initial beam jet direction, and increase with increasing off-shellness. Unlike conventional showers, the splitting function $\mathcal{P}$ depends on transverse momenta and includes part of the virtual corrections, in such a way as to avoid double counting with the Sudakov form factor while reconstructing color coherence in the small-x region (5).

The Monte Carlo also contains time-like parton showering. The impact of time-like showers on the jet observables that we will examine in this section turns out to be very small. This is similar to what is found in the studies [17, 18] of Tevatron di-jets and $\Delta\phi$

distribution, based on HERWIG and PYTHIA. See remark toward the beginning of Sec. II. Some details on the treatment of time-like showering effects are reported in Appendix B. A more complete account of this topic may be found in [61].

D. Azimuthal jet distributions

The $k_\perp$-dependent ME and parton branching lead to a different angular pattern of initial-state gluon radiation than standard, collinear-based showers, e.g. HERWIG. In particular, while the HERWIG angular ordering reduces to ordering in transverse momenta for $x \to 0$, the $k_\perp$-dependent shower contains finite-angle corrections in this limit [11]. We now compute angular distributions for the ep three-jet cross section by the $k_\perp$-shower Monte Carlo CASCADE and by HERWIG. Let $\Delta\phi$ be the azimuthal separation between the two jets with

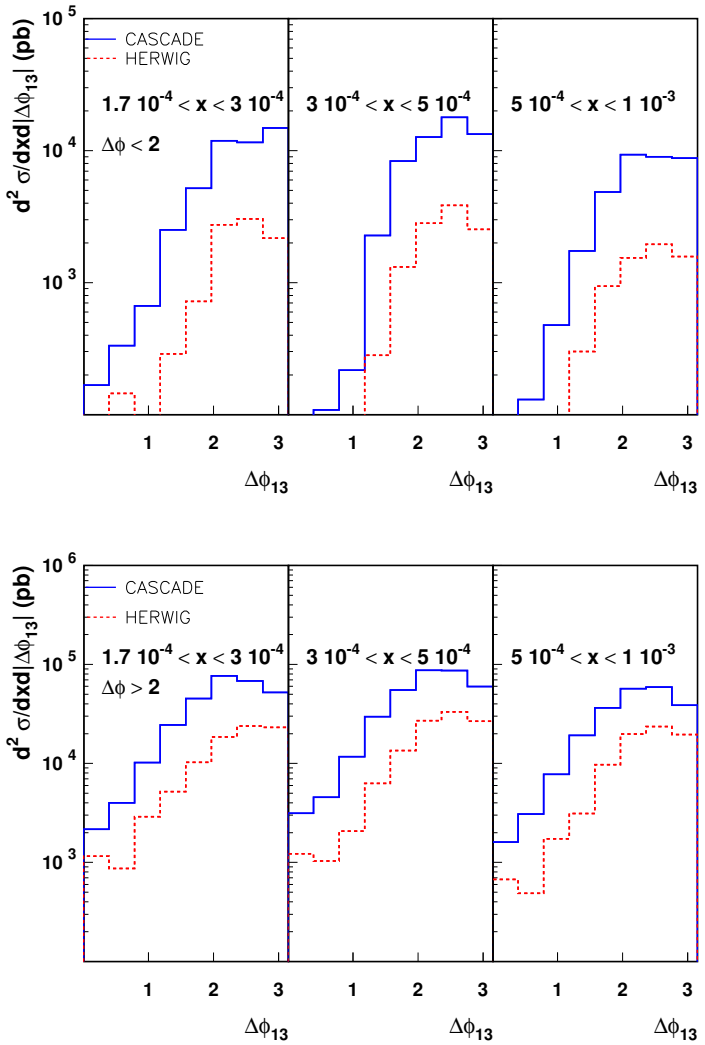

FIG. 5: Cross section in the azimuthal angle $\Delta\phi_{13}$ between the hardest and the 3rd jet for small ($\Delta\phi < 2$, top) and large ($\Delta\phi > 2$, bottom) azimuthal separations between the leading jets. The $k_\perp$Monte Carlo results CASCADE are compared with HERWIG.

the highest transverse energy E_T,

$$\Delta\phi = \phi_{\mathrm{jet}-1} - \phi_{\mathrm{jet}-2} \ , \tag{6}$$

where the azimuthal angle ϕ for each jet is defined in the hadronic center-of-mass frame. Similarly, we define $\Delta\phi_{13}$ as the azimuthal separation between the hardest and the third jet.

In Fig. 5 we compute the three-jet cross section and plot it versus the azimuthal angle $\Delta\phi_{13}$, by distinguishing the cases in which the two leading jets are at small angular separation ($\Delta\phi < 2$) or large angular separation ($\Delta\phi > 2$). CASCADE gives large differences from HERWIG in the region where the azimuthal separations $\Delta\phi$ between the leading jets are small, see top plot of Fig. 5. This reflects the fact that at small $\Delta\phi$ the phase space opens

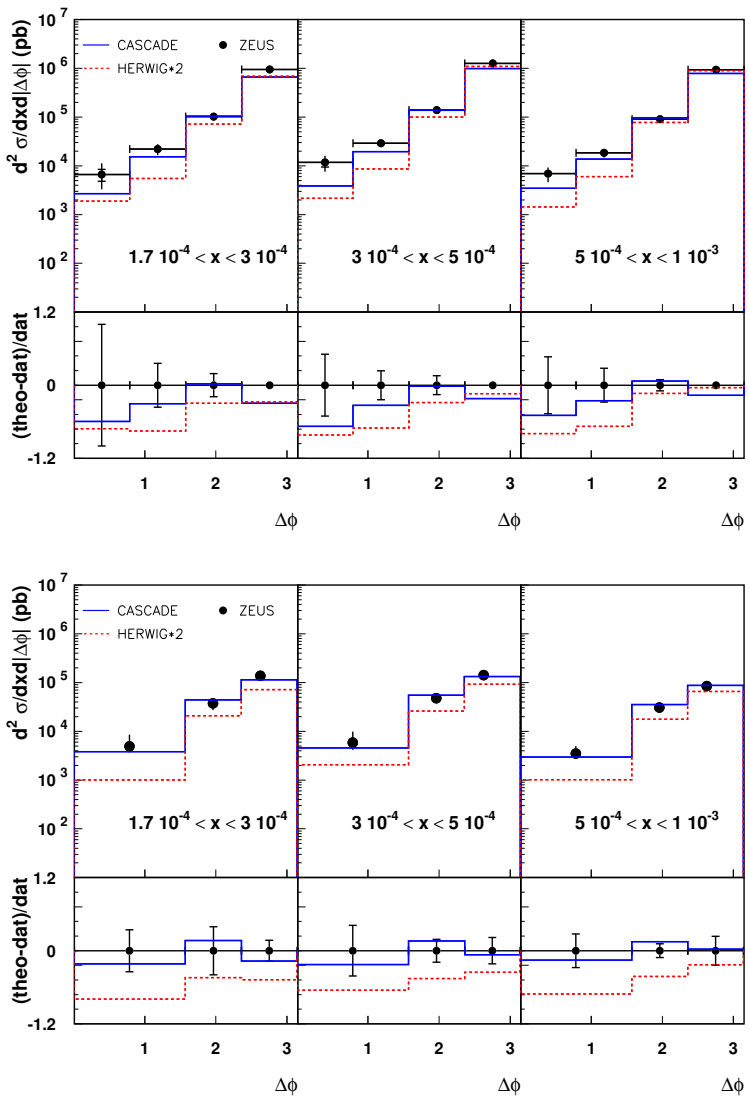

FIG. 6: Angular jet correlations obtained by the $k_\perp$-shower CASCADE and by HERWIG, compared with ep data [16]: (top) di-jet cross section; (bottom) three-jet cross section. The HERWIG results are multiplied by a factor of 2.

up for events in which the partonic lines along the initial decay chain are not ordered in transverse momentum. Such configurations are taken into account in CASCADE with the appropriate matrix element, at least for small enough x, but not in HERWIG. The x values

considered in Fig. 5 are those corresponding to the three-jet measurements in [16]. As $\Delta\phi$ increases, the results from CASCADE and HERWIG become closer. See bottom plot of Fig. 5. This is associated with the fact that for $\Delta\phi$ approaching the back-to-back region the phase space for finite-$k_\perp$emissions is reduced. In this region one thus expects both Monte Carlos to give reasonable approximations.

Fig. 6 shows the angular correlations for final states with two jets and three jets. We compute the azimuthal distribution of di-jet and three-jet cross sections in the separation $\Delta\phi$ between the leading jets. We show the distributions obtained by CASCADE and by HERWIG, compared with the measurement [16]. We multiply the HERWIG result by a constant factor equal to 2, which the top plot in Fig. 6 shows is the K-factor needed in order to get the normalization approximately correct for the two-jet region. Observe that the shape of the distribution is different for the two Monte Carlos. As expected from the result of Fig. 5, CASCADE gives the largest differences to HERWIG at small $\Delta\phi$, and becomes closer to HERWIG as $\Delta\phi$ increases. In particular, we observe that while the K-factor of 2 for HERWIG is sufficient for the two-jet region, the shape of the jet distribution is not properly described by HERWIG as $\Delta\phi$ decreases. The description of the measurement by CASCADE is good, whereas HERWIG is not sufficient to describe the measurement in the small $\Delta\phi$ region. We further see in the bottom plot of Fig. 6 that the three-jet cross section is reasonably well described by the $k_\perp$-shower result but not by HERWIG.

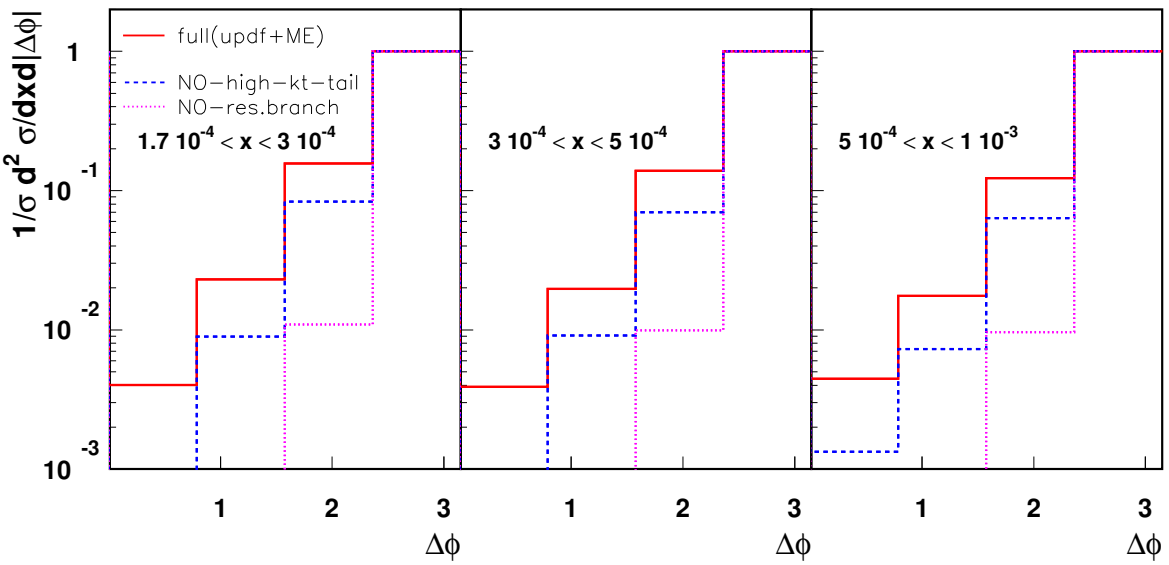

FIG. 7: Azimuthal distribution normalized to the back-to-back cross section: (solid red) full result (u-pdf $\oplus$ ME); (dashed blue) no finite-$k_\perp$correction in ME (u-pdf $\oplus$ ME$_{collin.}$); (dotted violet) u-pdf with no resolved branching.

Note that the interpretation of the angular correlation data in terms of corrections to collinear ordering is consistent with the finding [16] discussed in Sec. II that while inclusive jet rates are reliably predicted by NLO fixed-order results, NLO predictions are affected by large corrections to di-jet azimuthal distributions (going from $\mathcal{O}(\alpha_s^2)$ to $\mathcal{O}(\alpha_s^3)$) in the small-$\Delta\phi$ and small-x region, and begin to fall below the data for three-jet distributions in

the smallest $\Delta\phi$ bins (Fig. 3 [16]).

The physical picture underlying the $k_\perp$-shower calculation in Figs. 5,6 involves both transverse-momentum dependent parton distributions (determined from experiment) and matrix elements (computed perturbatively). Fig. 7 illustrates the relative contribution of these different components to the result, showing different approximations to the azimuthal dijet distribution normalized to the back-to-back cross section. The solid red curve is the full result. The dashed blue curve is obtained from the same unintegrated pdf's but by taking the collinear approximation in the hard matrix element,

$$\mathcal{M}(k_\perp) \to \mathcal{M}_{collin.}(k_\perp) = \mathcal{M}(0_\perp)\ \Theta(\mu - k_\perp)\ . \tag{7}$$

The dashed curve drops much faster than the full result as $\Delta\phi$ decreases, indicating that the high-$k_\perp$component in the hard ME [10] is necessary to describe jet correlations for small $\Delta\phi$ [62]. For reference we also plot, with the dotted (violet) curve, the result obtained from the unintegrated pdf without any resolved branching,

$$\mathcal{A}(x, k_\perp, \mu) \to \mathcal{A}_{no-res.}(x, k_\perp, \mu) = \mathcal{A}_0(x, k_\perp, Q_0)\ \Delta(\mu, Q_0) \quad . \tag{8}$$

Here $\mathcal{A}_0$ is the starting distribution at Q_0 and Δ is the Sudakov form factor, giving the no-radiation probability between Q_0 and μ. This represents the contribution of the intrinsic $k_\perp$distribution only, corresponding to nonperturbative, predominantly low-$k_\perp$modes. That is, in the dotted (violet) curve one retains an intrinsic $k_\perp \neq 0$ but no effects of coherence. We see that the resulting jet correlations in this case are down by an order of magnitude.

The results of Fig. 7 illustrate that the $k_\perp$-dependence in the unintegrated pdf alone is not sufficient to describe jet production quantitatively, and that jet correlations are sensitive to the finite, high-$k_\perp$tail of matrix elements [10] computed from perturbation theory. We note that the inclusion of the perturbatively computed high-k$_\perp$ correction distinguishes the present calculation of multi-jet cross sections from other shower approaches (see e.g. [15]) that include transverse momentum dependence in the pdfs but not in the matrix elements.

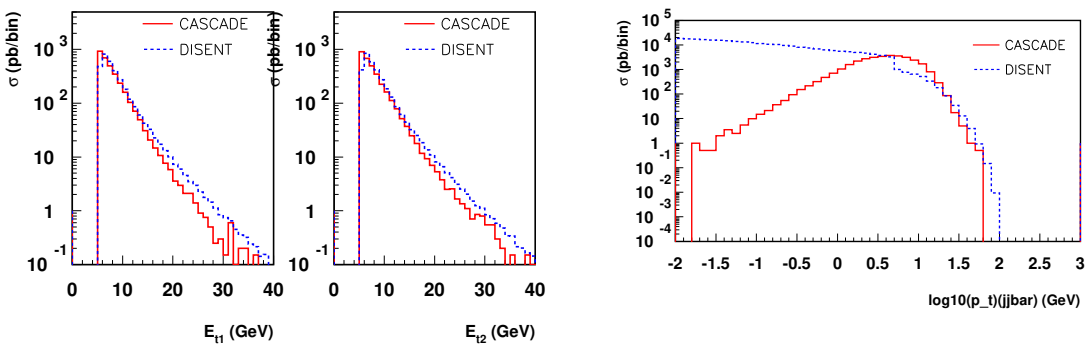

FIG. 8: Comparison of the k$_\perp$-shower CASCADE with the NLO di-jet calculation DISENT: (left) distribution in single-jet transverse energy; (right) distribution in the di-jet transverse energy.

To examine more closely the distribution in k$_\perp$ that results from highly off-shell subprocesses, in Fig. 8 we study the jet cross section in transverse energy and compare the k$_\perp$-shower with the NLO result from the DISENT event generator. It is noteworthy that the large-p_t part of the di-jet spectrum is very close for the two calculations. At low p_t one sees the Sudakov form-factor effect in the shower result. Differences in the single-jet spectra are also of interest and can be shown to be associated with quark contributions [61]. These

detailed comparisons may be of use to relate [63] DIS event shapes measuring the transverse momentum in the current region to hadro-production p_T spectra.

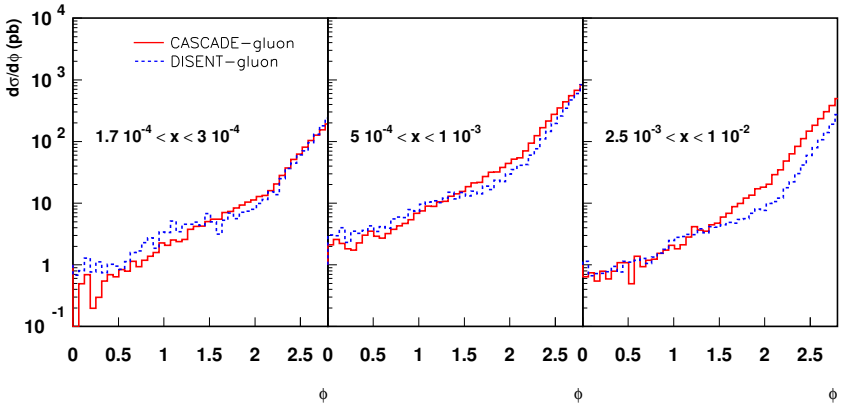

FIG. 9: Azimuthal di-jet distribution obtained from the expansion of the $k_\perp$-shower CASCADE to one-gluon emission level, compared with the NLO di-jet calculation DISENT(gluon channel).

In Fig. 9 we push further the comparison at next-to-leading-order level. We switch off hadronization, and use the $k_\perp$-shower Monte Carlo CASCADE as a parton-level generator. We evaluate the $k_\perp$-shower by expanding in the number of extra emissions, and truncate to the level of one gluon emission. We compare this with the NLO DISENT calculation, taking only the gluon channel in DISENT. We compute the azimuthal di-jet distribution at various values of x. The plots in Fig. 9 indicate that for sufficiently small x the one-gluon expansion of the shower program agrees with the full NLO result. We view this as a numerical consistency check of the shower program in the case of a relatively complicated final-state correlation, to be considered jointly with the analytic cross-checks quoted in Sec. III A, e.g. [34], for the case of analytic small-x results for inclusive observables.

We conclude this section by observing that the jets that we are considering are produced in the region of rapidities of Eq. (2), away from the forward region. While forward-region observables are relevant in their own right and have long been studied as probes of the initial-state shower dynamics (see e.g. [4, 28] and references therein), Monte Carlo results for such observables have a more pronounced dependence on the details of the model used for u-pdf evolution [11] (see also discussions in [27, 37, 48]). It is thus interesting that significant effects of non-ordering in $k_\perp$ for the space-like shower are found in the present case for centrally produced hard jets.

IV. JET MULTIPLICITIES AND MOMENTUM CORRELATIONS

We now turn to jet multiplicities and transverse-momentum correlations. These observables provide further details on the structure of the multi-jet final states. As noted in Sec. II, several of the transverse-momentum correlations measured in [16] are affected by sizeable theory uncertainties at NLO [16, 21].

Let us first consider jet multiplicity distributions. Finite-$k_\perp$ corrections increase the mean gluon multiplicity and broaden the spectrum [8–10]. In Fig. 10 we compute the distribution in the number of jets N, normalized to the two-jet cross section σ. As in Fig. 5 we show

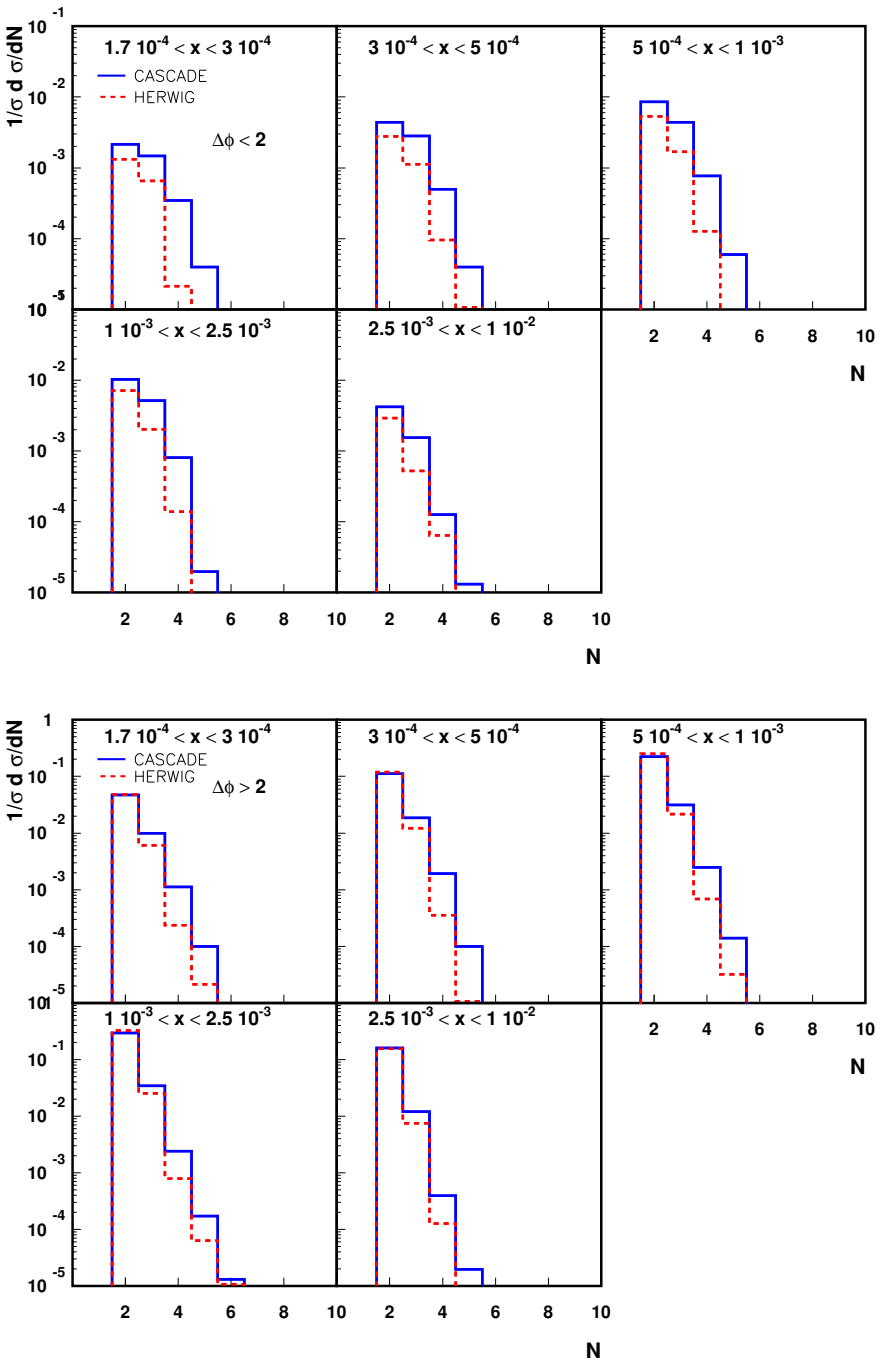

FIG. 10: Jet multiplicities obtained by CASCADE and HERWIG for (top) $\Delta\phi < 2$ and (bottom) $\Delta\phi > 2$.

separately the results for small and large azimuthal separations between the hardest jets, $\Delta\phi < 2$ and $\Delta\phi > 2$. Jet multiplicities at small $\Delta\phi$ are where the clearest differences appear between the two parton showers. The $k_\perp$-shower result receives larger contribution from high multiplicities. Besides the absolute size of this contribution, note that Fig. 10 illustrates the difference in the shape between the two Monte Carlos.

In Ref. [16] the ZEUS collaboration has presented measurements of various momentum correlations. We examine two such distributions for three-jet cross sections in Figs. 11 and

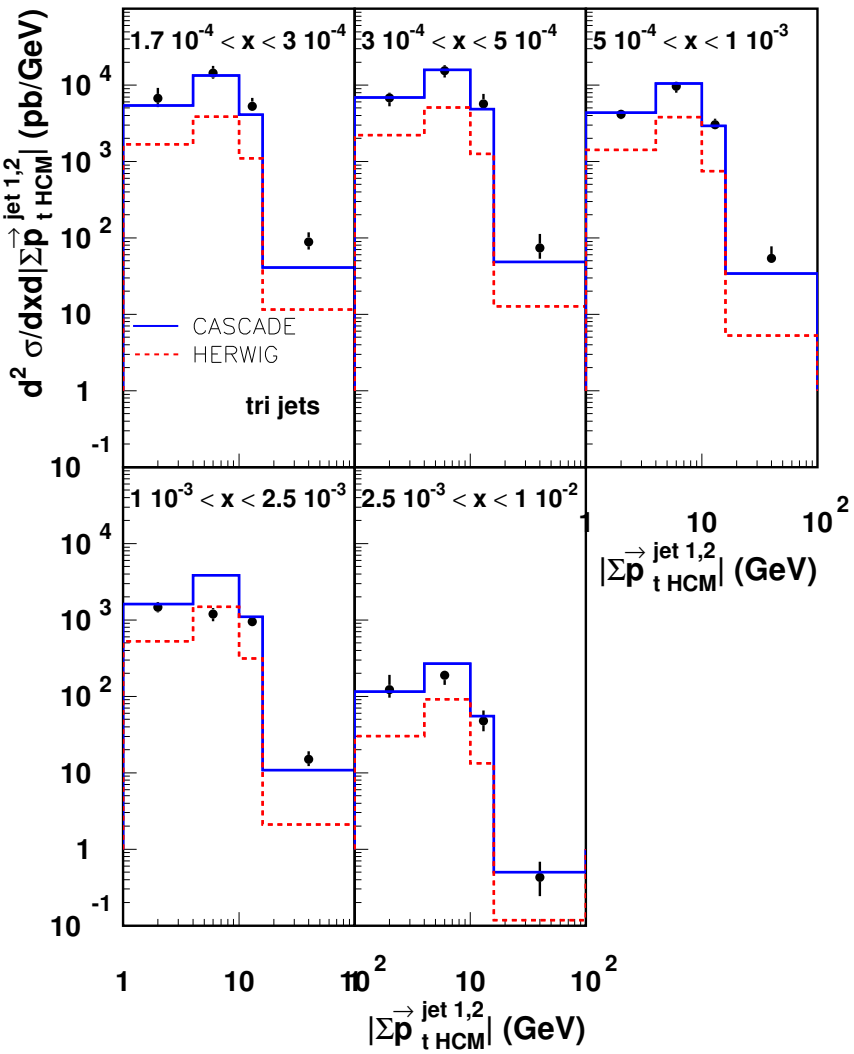

FIG. 11: Momentum correlations obtained by CASCADE and HERWIG, compared with ep data [16]: three-jet cross section versus the variable $|\sum p_T^{1,2}|$ introduced in the text.

12. In Fig. 11 is shown the distribution in the magnitude of the sum of the transverse momenta p_T for the two jets with the highest E_T, $|\sum p_T^{1,2}|$. The back-to-back region corresponds to $|\sum p_T^{1,2}| \to 0$ in this plot. The region of large $|\sum p_T^{1,2}|$ is the region with at least three well-separated hard jets. The $k_\perp$-shower result describes this region reasonably well. The results from HERWIG are quite lower.

In Fig. 12 is the distribution in the vector difference of the highest-E_T jet transverse momenta, scaled by twice the transverse energy of the hardest jet, $|\Delta p_T^{1,2}|/(2E_T^1)$. The back-to-back region corresponds to $|\Delta p_T^{1,2}|/(2E_T^1) \to 1$ in this plot. The behavior of the Monte Carlo results compared to the data is rather similar to that in Fig. 11.

In summary, the calculations of this paper show that the $k_\perp$-shower results describe well the shape of multi-jet distributions observed experimentally, including correlations, and give quite distinctive features of the associated distributions compared to standard showers such as HERWIG. The largest differences between the two parton showers occur when the

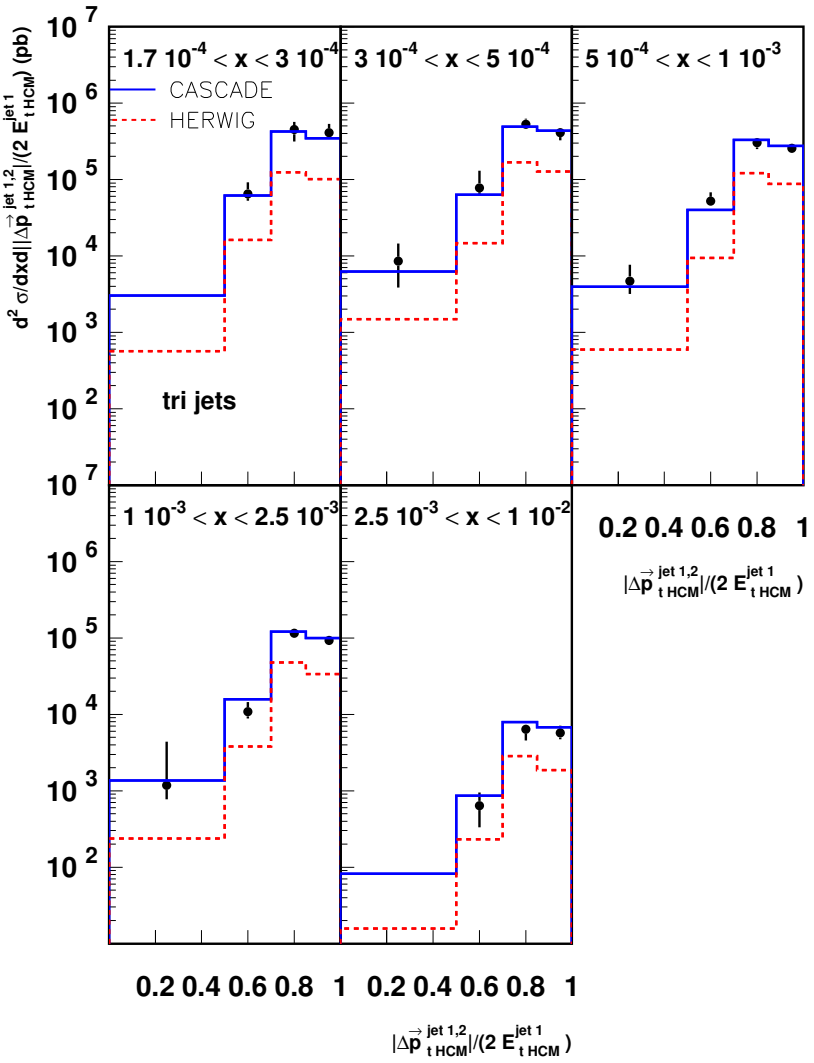

FIG. 12: Momentum correlations obtained by CASCADE and HERWIG, compared with ep data [16]: three-jet cross section versus the variable $|\Delta p_T^{1,2}|/(2E_T^1)$ introduced in the text.

azimuthal separations between the leading jets are small, whereas the results become more similar in the two-jet region. See e.g. Figs. 6,10. In the region of small azimuthal distances the largest variation occurs between order-α_s^2 and order-α_s^3 results in the fixed-order NLO calculations, particularly for small x. In cases where corrections are not large, the NLO and $k_\perp$-shower calculations are rather close. The results support a physical picture of multi-jet correlations in which sizeable radiative corrections arise not only from collinear/soft emission, included in HERWIG as well, but also from finite-angle emission, associated with the growth of transverse momenta transmitted along the space-like jet. Small-x coherence effects, computed in this section and the previous section for jet multiplicities, momentum correlations and angular correlations, are included in the $k_\perp$-shower but not in HERWIG. They are associated with multi-gluon radiation terms to the initial-state shower that become

non-negligible at high energy and small $\Delta\phi$.[6]

The above observations suggest the usefulness of combining NLO and $k_\perp$-shower for a broad range of multi-jet observables, in order to obtain more reliable predictions over a wider kinematic region. Monte Carlo results depend on the maximum angle parameter μ [8, 11, 12] at which the shower is evaluated. The perturbative matching will involve this angle. Studies of the dependence of Monte Carlo results on μ will be reported elsewhere.

V. PROSPECTS FOR LHC FINAL STATES AND CONCLUSIONS

Experimental analyses of multi-particle final states at the Large Hadron Collider depend on realistic parton-shower Monte Carlo simulations. Multi-particle production acquires qualitatively new features at the LHC compared to previous hadron-hadron experiments due to the large phase space opening up for events characterized by multiple hard scales, possibly widely disparate from each other. This brings in both potentially large radiative corrections and potentially new effects in the nonperturbative components of the process being probed near phase-space boundaries. It is not at all obvious that the approximations involved in standard Monte Carlo generators that have successfully served for event simulation in past collider experiments will be up to the new situation.

In this paper we have discussed the method of $\mathrm{k}_\perp$-dependent Monte Carlo shower, based on transverse-momentum dependent (TMD), or unintegrated, parton distributions and matrix elements defined by high-energy factorization. The main advantage of the method over standard Monte Carlo generators is the inclusion of corrections to collinear-ordered showers, and of effects of QCD coherence associated with finite-angle radiation from space-like partons carrying arbitrarily soft longitudinal momenta. Sensitivity to these dynamical features is bound to be enhanced by the high-energy multi-scale kinematics. The theoretical basis of the $\mathrm{k}_\perp$-shower method allows one to go to arbitrarily high transferred-momentum scales, thus making it suitable for event simulation of jet physics at the LHC.

In the paper we have pointed to developments of the approach toward general-purpose event generators, and illustrated validation of $\mathrm{k}_\perp$-shower Monte Carlo using experimental ep data for final states with multiple hadronic jets. We have noted that while Tevatron di-jet correlations are dominated by leading-order processes, and are reasonably well described by collinear-based event generators, this is not so in the case of ep data. We have found that including finite-$\mathrm{k}_\perp$ radiative contributions in the initial state shower gives sizeable effects and improves significantly the description of angular correlations and transverse-momentum correlations. Despite the lower ep energy, the multi-jet kinematic region considered is characterized by the large phase space available for jet production and relatively small values of the ratio between the jet transverse momenta and center-of-mass energy, and is thus relevant for extrapolation of initial-state showering effects to the LHC.

Besides jet final states, the corrections to collinear-ordered showers that we are treating will also affect heavy mass production at the LHC, including final states with heavy bosons and heavy flavor. An example is provided by bottom-quark pair production. Going from the Tevatron to the LHC [64] implies a sharp increase in the relative fraction of events dominated by the $g \to b\bar{b}$ subprocess coupling [10] to the spacelike jet. This is bound to affect the

[6] Near the back-to-back region of large $\Delta\phi$, on the other hand, corrections due to mixed Coulomb/radiative terms can also become important [39, 40].

reliability of shower calculations based on collinear ordering (as well as the stability of NLO perturbative predictions), as these do not properly account for contributions of $b\bar{b}$ in association with two hard jets, with p_t of the heavy quark pair large compared to the bottom-quark mass but small compared to the transverse momenta of the individual associated jets. These kinematic regions are the analogue of the regions unordered in $k_\perp$ studied in this paper for jet correlations. The fraction of $b\bar{b}$ events of this kind is not very significant at the Tevatron but will be sizeable at the LHC. The quantitative importance of unordered configurations coupling to $g \to b\bar{b}$ will reduce the numerical stability of collinear-based predictions (NLO, or parton-shower, or their combination [65]) with respect to renormalization/factorization scale variation in the case of LHC. On the other hand, these are precisely the configurations that the $k_\perp$ Monte Carlo shower is designed to treat.

Even more complex multi-scale effects are to be expected, and are beginning to be investigated [61], in the associated production of bottom quark pairs and W/Z bosons [66], and possibly in final states with Higgs bosons [33, 67][7] especially for measurements of the less inclusive distributions and correlations. The vector boson case is relevant for early phenomenology at the LHC, as small-x broadening of W and Z p_T distributions [69] (see [70]) affects the use of these processes as luminosity monitor [71].

The $k_\perp$-shower method discussed in this paper can be used all the way up to high transferred-momentum scales. As an illustration in Fig. 13 we present a numerical calculation for the transverse momentum spectrum of top-antitop pair production at the LHC. Small-x effects are not large in this case. Rather, this process illustrates how the shower works in the region of finite x and large virtualities on the order of the top quark mass. It is interesting to note that even at LHC energies the transverse momentum distribution of top quark pairs calculated from the $k_\perp$-shower is similar to what is obtained from a full NLO calculation (including parton showers, MC@NLO [65]), with the $k_\perp$-shower giving a somewhat harder spectrum, Fig. 13.

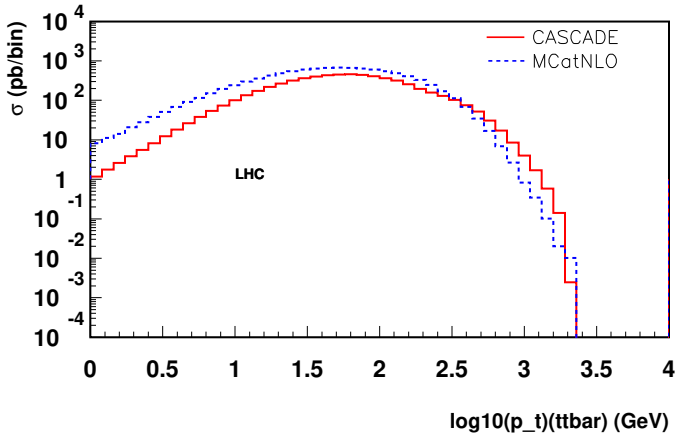

FIG. 13: Comparison of transverse momentum distribution of $t\bar{t}$ pairs calculated from the $k_\perp$-shower CASCADE with the NLO calculation MC@NLO at LHC energies.

We conclude by observing that using off-shell matrix elements convoluted with unin-

[7] Non-negligible numerical effects of high-energy subleading terms were noted [68] in the predictions for the Higgs transverse-momentum spectrum at the LHC.

tegrated parton distributions including explicit parton showering, many of the subleading effects are properly simulated both in ep collisions and at the LHC. We have found that multi-jet predictions provide comparable results to NLO calculations, where applicable, and are much closer to the measurements in a region where significant higher order contributions are expected. The results provide a strong motivation for systematic studies of $k_\perp$-dependent parton branching methods.

Acknowledgments. We are grateful to S. Chekanov for many discussions about the jet measurements. We gratefully acknowledge useful discussions with Z. Nagy and A. Savin. Thanks to the HERA machine crew and experiments for providing precise and interesting measurements of multi-jet correlations. Part of this work was done while one of us (F.H.) was visiting DESY. We thank the DESY directorate for hospitality and support.

APPENDIX A: FITS TO THE STARTING PDFS

The branching equations (3),(4) contain the starting gluon distribution $\mathcal{A}_0(x, k_\perp, Q_0)$ at scale Q_0. This is determined from fits to experimental data. In this appendix we report

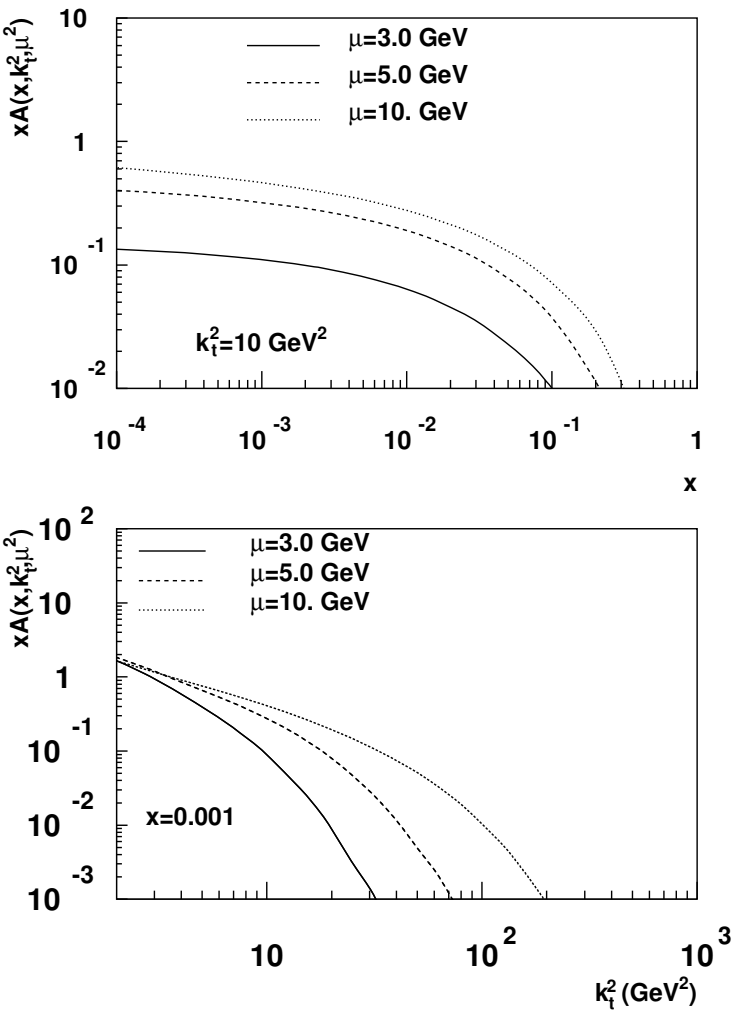

FIG. 14: (top) x-dependence and (bottom) $k_\perp$-dependence of the unintegrated gluon distribution at different values of the evolution scale μ.

results for this distribution.

The starting $\mathcal{A}_0(x, k_\perp, Q_0)$ at scale Q_0 is parameterized as [11, 33]

$$x\mathcal{A}_0(x, k_\perp, Q_0) = A\ x^{-B}\ (1-x)^C\ \exp\left[-(k_\perp - \lambda)^2/\nu^2\right] \quad . \tag{A1}$$

The values of the parameters A, B, C, λ and ν in Eq. (A1) are determined from data fits [33, 72]. In the calculations of the present paper we use the u-pdf set specified by the following parameter values:

$$\begin{aligned} Q_0 \;&=\; 1.1 \text{ GeV} \quad , \quad A = 0.4695 \quad , \quad B = 0.025 \quad , \\ C \;&=\; 4.0 \quad , \quad \lambda = 1.5 \text{ GeV} \quad , \quad \nu = (1.5/\sqrt{2}) \text{ GeV} \quad . \end{aligned} \tag{A2}$$

In Fig. 14 we plot the x-dependence and $k_\perp$-dependence of the resulting gluon distribution at different values of the evolution scale μ.

APPENDIX B: TIME-LIKE SHOWERING EFFECTS

The partons from the initial state cascade are allowed to develop a time-like shower in CASCADE 2.0.2, to be published in [61]. Full details will be reported in this publication. To give an idea of the effects, we include one of the results in this appendix.

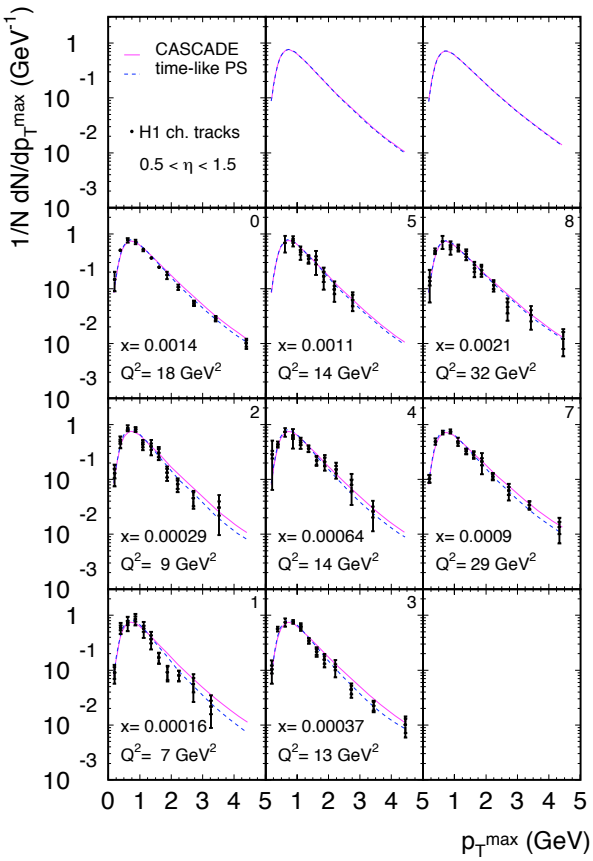

FIG. 15: The effect of including time-like showering on the ep charged-particle spectrum, along with the data [73].

The maximum scale for the time-like cascade is given by the transverse momentum of the initial state gluon. No additional constraints are applied to the time-like shower. It is found that the number of gluons after the initial state cascade with time-like showering increases; however the effect on the angular correlations considered in Sec. III of this paper is negligible (and smaller than the statistical error of the Monte Carlo simulation).

In observables which are more sensitive to the time-like showering, like the charged-particle transverse momentum spectra (Fig. 15), a small effect coming from the time-like showering can be observed, and is of the same size as that obtained from Monte Carlo event generators using the collinear parton-showering approach.

---

[1] Z. Bern *et al.*, arXiv:0803.0494 [hep-ph], in Proceedings of the Workshop "Physics at TeV Colliders" (Les Houches, 2007).

[2] S. Höche, F. Krauss, N. Lavesson, L. Lönnblad, M. Mangano, A. Schälicke and S. Schumann, hep-ph/0602031; N. Lavesson and L. Lönnblad, arXiv:0712.2966 [hep-ph].

[3] J. Alwall *et al.*, Eur. Phys. J. C **53** (2008) 473 [arXiv:0706.2569 [hep-ph]].

[4] S. Alekhin *et al.*, hep-ph/0601012, hep-ph/0601013: Proceedings of the Workshop "HERA and the LHC", eds. A. De Roeck and H. Jung.

[5] F. Hautmann and H. Jung, arXiv:0712.0568 [hep-ph].

[6] G. Corcella *et al.*, JHEP **0101** (2001) 010 [arXiv:hep-ph/0011363]; G. Corcella *et al.*, arXiv:hep-ph/0210213.

[7] T. Sjöstrand, S. Mrenna and P. Skands, JHEP **0605** (2006) 026.

[8] G. Marchesini and B.R. Webber, Nucl. Phys. **B386** (1992) 215.

[9] M. Ciafaloni, Nucl. Phys. **B296** (1988) 49.

[10] S. Catani, M. Ciafaloni and F. Hautmann, Phys. Lett. B **242** (1990) 97; Nucl. Phys. B**366** (1991) 135; Phys. Lett. B **307** (1993) 147.

[11] B. Andersson *et al.*, Eur. Phys. J. C **25** (2002) 77 [arXiv:hep-ph/0204115].

[12] H. Jung, Comput. Phys. Commun. **143** (2002) 100 [arXiv:hep-ph/0109102]; H. Jung and G.P. Salam, Eur. Phys. J. C **19** (2001) 351 [arXiv:hep-ph/0012143].

[13] L. Lönnblad and M. Sjödahl, JHEP **0505** (2005) 038; JHEP **0402** (2004) 042; G. Gustafson, L. Lönnblad and G. Miu, JHEP **0209** (2002) 005.

[14] K. Golec-Biernat, S. Jadach, W. Placzek, P. Stephens and M. Skrzypek, hep-ph/0703317.

[15] S. Höche, F. Krauss and T. Teubner, arXiv:0705.4577 [hep-ph].

[16] S. Chekanov *et al.* [ZEUS Collaboration], Nucl. Phys. B **786** (2007) 152 [arXiv:0705.1931 [hep-ex]].

[17] V.M. Abazov *et al.* [D0 Collaboration], Phys. Rev. Lett. **94** (2005) 221801 [arXiv:hep-ex/0409040].

[18] M.G. Albrow *et al.* [TeV4LHC QCD Working Group], arXiv:hep-ph/0610012.

[19] A. Aktas *et al.* [H1 Collaboration], Eur. Phys. J. C **33** (2004) 477 [arXiv:hep-ex/0310019].

[20] M. Hansson [H1 Collaboration], in Proceedings of the 14th International Workshop on Deep Inelastic Scattering DIS2006 (Tsukuba, April 2006), p. 539.

[21] Z. Nagy and Z. Trocsanyi, Phys. Rev. Lett. **87** (2001) 082001 [arXiv:hep-ph/0104315].

[22] C. Adloff *et al.* [H1 Collaboration], Eur. Phys. J. C **19** (2001) 269 [arXiv:hep-ex/0012052].

[23] Y. Delenda, R. Appleby, M. Dasgupta and A. Banfi, JHEP **0612** (2006) 044 [arXiv:hep-ph/0610242].

[24] A. Banfi and M. Dasgupta, JHEP **0401** (2004) 027.

[25] Y. Delenda, arXiv:0706.2172; A. Banfi, M. Dasgupta and Y. Delenda, arXiv:0804.3786.

[26] J.C. Collins, talk at the Light Cone 2008 Workshop, Mulhouse, July 2008 [arXiv:0808.2665 [hep-ph]].

[27] J.C. Collins, hep-ph/0106126, in Proceedings of the Workshop DIS01 (Bologna, 2001).

[28] J.R. Andersen *et al.*, Eur. Phys. J. C **35** (2004) 67.
[29] M. Ciafaloni, talk at RADCOR2007, Florence, October 2007.
[30] G. Altarelli, talk at RADCOR2007, Florence, October 2007 [arXiv:0802.0968 [hep-ph]].
[31] S. Catani and F. Hautmann, Nucl. Phys. **B427** (1994) 475; Phys. Lett. B **315** (1993) 157.
[32] L.N. Lipatov, Phys. Rept. **286** (1997) 131.
[33] H. Jung, Mod. Phys. Lett. A**19** (2004) 1.
[34] M. Buza, Y. Matiounine, J. Smith, R. Migneron and W.L. van Neerven, Nucl. Phys. **B472** (1996) 611; S. Riemersma, W.L. van Neerven and J. Smith, Phys. Lett. B **347** (1995) 143; E. Laenen, S. Riemersma, W.L. van Neerven and J. Smith, Nucl. Phys. **B392** (1993) 162.
[35] S. Moch, J.A.M. Vermaseren and A. Vogt, Phys. Lett. B **606** (2005) 123; Nucl. Phys. **B691** (2004) 129.
[36] J.C. Collins and F. Hautmann, Phys. Lett. B **472** (2000) 129.
[37] T.C. Rogers, arXiv:0807.2430 [hep-ph]; arXiv:0712.1195 [hep-ph], in Proceedings of the 8th International Symposium on Radiative Corrections RADCOR2007 (Florence, October 2007); J.C. Collins, T.C. Rogers and A.M. Stasto, arXiv:0708.2833 [hep-ph].
[38] J.C. Collins, D.E. Soper and G. Sterman, Nucl. Phys. B**308** (1988) 833.
[39] J.C. Collins, arXiv:0708.4410 [hep-ph].
[40] W. Vogelsang and F. Yuan, Phys. Rev. D **76** (2007) 094013.
[41] C.J. Bomhof and P.J. Mulders, Nucl. Phys. B**795** (2008) 409.
[42] J.R. Forshaw, A. Kyrieleis and M.H. Seymour, JHEP **0608** (2006) 059; M.H. Seymour, arXiv:0710.2733 [hep-ph].
[43] F. Hautmann, Phys. Lett. B **655** (2007) 26.
[44] G.P. Korchemsky and A. Radyushkin, Phys. Lett. B **279** (1992) 359, G.P. Korchemsky and G. Marchesini, Phys. Lett. B **313** (1993) 433.
[45] I.O. Cherednikov and N.G. Stefanis, Nucl. Phys. B**802** (2008) 146; Phys. Rev. D **77** (2008) 094001; arXiv:0711.1278 [hep-ph].
[46] J.C. Collins, in *Perturbative Quantum Chromodynamics*, ed. A.H. Mueller, World Scientific 1989, p. 573.
[47] M. Anselmino et al., arXiv:0807.0173 [hep-ph]; M. Anselmino et al., Phys. Rev. D **71** (2005) 074006.
[48] F. Ceccopieri and L. Trentadue, Phys. Lett. B **660** (2008) 43.
[49] A. Bacchetta, D. Boer, M. Diehl and P.J. Mulders, arXiv:0803.0227 [hep-ph].
[50] Y. Koike, W. Vogelsang and F. Yuan, Phys. Lett. B **659** (2008) 878; and references therein.
[51] S. Meissner, K. Goeke, A. Metz and M. Schlegel, arXiv:0805.3165 [hep-ph]; and references therein.
[52] J.C. Collins and F. Hautmann, JHEP **0103** (2001) 016; F. Hautmann, hep-ph/0101006.
[53] X. Ji, J. Ma and F. Yuan, Phys. Rev. D **71** (2005) 034005, JHEP **0507** (2005) 020.
[54] A.V. Manohar and I.W. Stewart, Phys. Rev. D **76** (2007) 074002.
[55] C. Lee and G. Sterman, Phys. Rev. D **75** (2007) 014022.
[56] A. Idilbi and T. Mehen, Phys. Rev. D **75** (2007) 114017.
[57] C.W. Bauer, F.J. Tackmann and J. Thaler, arXiv:0801.4028; arXiv:0801.4026.
[58] J. Chay, arXiv:0711.4295.
[59] C.W. Bauer, S.P. Fleming, C. Lee and G. Sterman, arXiv:0801.4569 [hep-ph]; J. Chiu, F. Golf, R. Kelley and A.V. Manohar, Phys. Rev. D **77** (2008) 053004; M.D. Schwartz, Phys. Rev. D **77** (2008) 014026; M. Trott, Phys. Rev. D **75** (2007) 054011.
[60] F. Hautmann, arXiv:0708.1319 [hep-ph].

[61] M. Deak, H. Jung et al., contribution to HERA-LHC 2008 Proceedings; in progress.
[62] F. Hautmann and H. Jung, arXiv:0804.1746 [hep-ph], in Proceedings of the 8th International Symposium on Radiative Corrections RADCOR2007 (Florence, October 2007).
[63] M. Dasgupta and Y. Delenda, JHEP **0608** (2006) 080.
[64] J. Baines et al., Report of the Heavy Quark Working Group, arXiv:hep-ph/0601164; P. Nason et al., Report on bottom production, in "SM physics at the LHC", arXiv:hep-ph/0003142.
[65] S. Frixione, P. Nason and B. R. Webber, JHEP **0308** (2003) 007 [arXiv:hep-ph/0305252].
[66] M.L. Mangano, Nucl. Phys. B **405** (1993) 536.
[67] F. Hautmann, Phys. Lett. B **535** (2002) 159.
[68] A. Kulesza, G. Sterman and W. Vogelsang, Phys. Rev. D **69** (2004) 014012.
[69] F.I. Olness, talk at HERA-LHC Workshop, CERN, May 2008.
[70] S. Berge, P.M. Nadolsky, F.I. Olness and C.P. Yuan, hep-ph/0508215; P.M. Nadolsky, N. Kidonakis, F.I. Olness and C.P. Yuan, Phys. Rev. D **67** (2003) 074015.
[71] A.M. Cooper-Sarkar, arXiv:0707.1593 [hep-ph].
[72] M. Hansson and H. Jung, arXiv:0707.4276 [hep-ph].
[73] C. Adloff *et al.* [H1 Collaboration], Nucl. Phys. B **485** (1997) 3 [arXiv:hep-ex/9610006].